Recent Developments in HOMME Dynamical Core

Ram D. Nair

Computational Information Systems Laboratory / IMAGe
National Center for Atmospheric Research, Boulder, CO

[CESM Atmosphere Model Working Group Meeting,
Feb. 8–10th, 2016, NCAR, Boulder, Colorado]

NCAR

The HOMME DyCore Framework

- Horizontal Grid system (Cubed-Sphere)

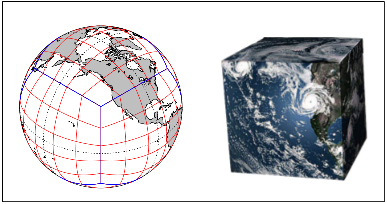

- Governing Equations (η-coordinate)

$$\begin{aligned}
\frac{\partial \mathbf{v}}{\partial t} + (f+\zeta)\hat{\mathbf{k}}\times\mathbf{v} + \dot{\eta}\frac{\partial \mathbf{v}}{\partial \eta} + \nabla E + \frac{RT_v}{p}\nabla p &= \mathbf{F}_v \\
\frac{\partial T}{\partial t} + \mathbf{v}\cdot\nabla T + \dot{\eta}\frac{\partial T}{\partial \eta} - \frac{R}{c_p^*}T_v\frac{\omega}{p} &= F_T \\
\frac{\partial}{\partial t}\left(\frac{\partial p}{\partial \eta}\right) + \nabla\cdot\left(\mathbf{v}\frac{\partial p}{\partial \eta}\right) + \frac{\partial}{\partial \eta}\left(\dot{\eta}\frac{\partial p}{\partial \eta}\right) &= 0 \\
\frac{\partial}{\partial t}\left(\frac{\partial p}{\partial \eta}q_k\right) + \nabla\cdot\left(\frac{\partial p}{\partial \eta}\mathbf{v}q_k\right) + \frac{\partial}{\partial \eta}\left(\dot{\eta}\frac{\partial p}{\partial \eta}q_k\right) &= 0
\end{aligned}$$

- HOMME hydrostatic framework is based on cubed-sphere geometry (Sadourny, 1972). Sepctral Element (SE) and discontinuous Galerkin (DG) methods are used for spatial discretization
- Quasi-uniform rectangular mesh with local refinement capability, well suited for SE, DG or FV methods.
- HOMME-SE variant is used in CAM framework (CAM-SE) as a default dycore. Explit time-stepping and proven petascale capability (Dennis et al. 2012).

- HOMME currently employs pressure-based η-coordinates in the vertical with FD or VL discretization .
- Semi-Lagrangian FV scheme (CSLAM) for multi-tracer transport
- Hydrostatic dynamics is not suitable or valid for horizontal resolution less than 10 KM $(1/8^\circ)$

Toward a Non-Hydrostatic (NH) HOMME: Basic Design

- The NH model development in HOMME framework is named as the High-Order Multiscale Atmopsheric Model ("HOMAM")
- The dynamics is governed by 3D compressible Euler/Navier-Stokes system of equations, based on conservation of mass, energy, momentum etc.

- 3D Compressible Euler system (flux-form) on a rotating sphere

$$
\begin{aligned}
\frac{\partial \rho}{\partial t} + \nabla \cdot (\rho \mathbf{V}) &= 0 \\
\frac{\partial \rho \mathbf{V}}{\partial t} + \nabla \cdot (\rho \mathbf{V} \otimes \mathbf{V}) &= -\nabla p' - (\rho - \overline{\rho}) g \mathbf{k} \\
&\quad -2\rho \Omega \times \mathbf{V} + \mathbf{F}_M \\
\frac{\partial \rho \theta}{\partial t} + \nabla \cdot (\rho \theta \mathbf{V}) &= 0 \\
\frac{\partial \rho q_k}{\partial t} + \nabla \cdot (\rho\, q_k \mathbf{V}) &= 0
\end{aligned}
$$

- $\mathbf{V} = (u, v, w)$ 3D wind field, ρ air density, p pressure, θ potential temperature, q_k moisture variables, Ω erath's rotation rate, f Coriolis term, $\mathbf{F}_M$ diffusive fluxes and forcing etc.
- Density $\rho = \overline{\rho} + \rho'$, and pressure $p = \overline{p} + p'$ such that the basic state follows hydrostatic balance, $\partial \overline{p} / \partial z = -\overline{\rho} g$.

Compressible Euler System in Generalized Coordinates

- The 3D compressible Euler system of equations on a rotating sphere in generalized curvilinear coordinates (x^1, x^2, x^3) can be written in tensor form (*Warsi, 1992*):

$$
\begin{aligned}
\frac{\partial \rho}{\partial t} + \frac{1}{\sqrt{G}}\left[\frac{\partial}{\partial x^j}(\sqrt{G}\rho u^j)\right] &= 0 \quad \{\text{Summation Implied}\} \\
\frac{\partial \rho u^i}{\partial t} + \frac{1}{\sqrt{G}}\left[\frac{\partial}{\partial x^j}[\sqrt{G}(\rho u^i u^j + p G^{ij})]\right] + \Gamma^i_{jk}(\rho u^j u^k + p G^{jk}) &= f\sqrt{G}(u^1 G^{2i} - u^2 G^{1i}) - \rho g G^{3i} \\
\frac{\partial \rho\theta}{\partial t} + \frac{1}{\sqrt{G}}\left[\frac{\partial}{\partial x^j}(\sqrt{G}\rho\theta u^j)\right] &= 0 \\
\frac{\partial \rho q}{\partial t} + \frac{1}{\sqrt{G}}\left[\frac{\partial}{\partial x^j}(\sqrt{G}\rho q u^j)\right] &= 0
\end{aligned}
$$

- Where u^i is contravariant wind field, G_{ij} metric tensor, $\sqrt{G} = |G_{ij}|^{1/2}$ is the Jacobian of the transform, $G^{ij} = (G_{ij})^{-1}$, and $i, j, k \in \{1, 2, 3\}$. The associated Christoffel symbols (second kind) are defined as

$$
\Gamma^i_{jk} = \frac{1}{2} G^{il}\left[\frac{\partial G_{kl}}{\partial x^j} + \frac{\partial G_{jl}}{\partial x^k} - \frac{\partial G_{kj}}{\partial x^l}\right]
$$

- ρ is the air density, q is the mixing ratio (passive tracer field).

Model Equations for the Cubed-Sphere Geometry

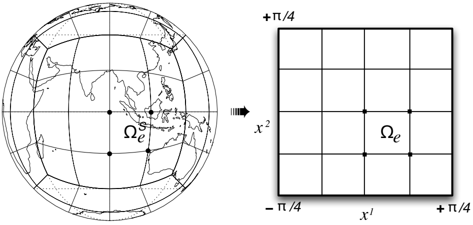

Physical Domain   Computational Domain

- Equiangular central projection
- Curvilinear horizontal coordinates (x^1, x^2)
- 6 patched domains, $x^1, x^2 \in [-\pi/4, \pi/4]$
- "Cartesian-like" computational domains

- Shallow (thin) atmosphere approximation makes the the spherical domain as a vertically stacked cubed-sphere layers.
- $x^3 = \text{radius}\, r + \text{ height}\, z$, s.t $\quad z \ll r \implies \quad (x^1, x^2, x^3) \rightarrow (x^1, x^2, z)$
- The metric tensor associated with shallow atmosphere takes a simple form,

$$G_{ij} = \begin{bmatrix} \hat{G}_{11} & \hat{G}_{12} & 0 \\ \hat{G}_{21} & \hat{G}_{22} & 0 \\ 0 & 0 & 1 \end{bmatrix}, \quad \hat{G}_{ij} = \frac{r^2}{\mu^4 \cos^2 x^1 \cos^2 x^2} \begin{bmatrix} 1 + \tan^2 x^1 & -\tan x^1 \tan x^2 \\ -\tan x^1 \tan x^2 & 1 + \tan^2 x^2 \end{bmatrix},$$

where $i, j \in \{1, 2\}$ and $\mu^2 = 1 + \tan^2 x^1 + \tan^2 x^2$. Jacobian $\sqrt{G_h} \equiv |G_{ij}|^{1/2} = |\hat{G}_{ij}|^{1/2}$

HOMAM: Vertical Grid System

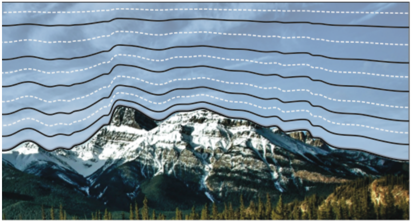

Fig Courtesy: David Hall

- Terrain-following height-based vertical z coordinate.
- Multiple options [e.g., Schär (2002), Klemp (2011), SLEVE]
- Vertical coordinate transformation (Gal-Chen & Somerville, JCP 1975), is currently adopted.

- $h_s = h_s(x^1, x^2)$ is the prescribed mountain profile and z_{top} is the top of the model domain

$$\zeta = z_{top}\frac{z - h_s}{z_{top} - h_s}, \quad z(\zeta) = h_s(x^1, x^2) + \zeta\,\frac{z_{top} - h_s}{z_{top}}; \quad h_s \le z \le z_{top}.$$

- The Jacobian associated with the transform $(x^1, x^2, z) \rightarrow (x^1, x^2, \zeta)$ is

$$\sqrt{G_v} = \left[\frac{\partial z}{\partial \zeta}\right]_{(x^1, x^2)} = 1 - \frac{h_s(x^1, x^2)}{z_{top}}$$

HOMAM: Vertical Coordinate Transform, $(x^1, x^2, z) \rightarrow (x^1, x^2, \zeta)$

- The vertical 'physical' velocity $w = dz/dt$, in (x^1, x^2, z) system
- Vertical velocity in the transformed (x^1, x^2, ζ) system is $u^3 = \tilde{w}$,

$$\tilde{w} = \frac{d\zeta}{dt}, \quad \sqrt{G_v}\tilde{w} = w + \sqrt{G_v}G_v^{13}\, u^1 + \sqrt{G_v}G_v^{23}\, u^2,$$

where (u^1, u^2) contravariant wind vectors on the cubed-sphere surface.
- Metric coefficients (*Clark 1977, JCP*)

$$\sqrt{G_v} = \left[\frac{\partial z}{\partial \zeta}\right]_{(x^1,x^2)}, \ \sqrt{G_v}G_v^{13} \equiv \left[\frac{\partial h_s}{\partial x^1}\right]_{(z)} \left(\frac{\zeta}{z_{top}} - 1\right), \quad \sqrt{G_v}G_v^{23} \equiv \left[\frac{\partial h_s}{\partial x^2}\right]_{(z)} \left(\frac{\zeta}{z_{top}} - 1\right).$$

- The spacial derivates for an arbitrary scalar ϕ can be written in terms of the transformed vertical ζ-coordinate as follows:

$$\sqrt{G_v}\frac{\partial \phi}{\partial z} = \frac{\partial \phi}{\partial \zeta}, \quad \sqrt{G_v}\frac{\partial \phi}{\partial x^i} = \frac{\partial(\sqrt{G_v}\phi)}{\partial x^i} + \frac{\partial(\sqrt{G_v}G_v^{i3}\phi)}{\partial \zeta}, \quad i = 1, 2.$$

HOMAM: 3D Transport Equation

- The transport equation in flux-from for a tracer variable q in 3D (x^1, x^2, z) coordinates can be written as

$$\frac{\partial \rho q}{\partial t} + \frac{1}{\sqrt{G_h}} \left[\frac{\partial}{\partial x^1}(\sqrt{G_h}\rho q u^1) + \frac{\partial}{\partial x^2}(\sqrt{G_h}\rho q u^2) + \frac{\partial}{\partial z}(\sqrt{G_h}\rho q w) \right] = 0$$

- Simplifications lead to logically "Cartesian-like" model equation. In computational ζ-coordinate this reduces to

$$\frac{\partial \psi}{\partial t} + \frac{\partial(\psi u^1)}{\partial x^1} + \frac{\partial(\psi u^2)}{\partial x^2} = -\frac{\partial(\psi \tilde{w})}{\partial \zeta},$$

  where the pseudo density $\psi = \sqrt{G}\rho q$, and $\sqrt{G} = \sqrt{G_h}\sqrt{G_v}$, is the "composite" Jacobian which combines the time-independent horizontal $(\sqrt{G_h})$ and the vertical $(\sqrt{G_v})$ metric terms.
- ρq is the conservative variable and $\tilde{w} = d\zeta/dt$ is the vertical velocity due to the coordinate transformation.

HOMAM: Governing Equations in (x^1, x^2, ζ) system

- Final form of the 'perturbed' Euler system in (x^1, x^2, ζ) 3D Cubed-sphere

$$\frac{\partial \mathbf{U}}{\partial t} + \frac{\partial \mathbf{F}_1}{\partial x^1} + \frac{\partial \mathbf{F}_2}{\partial x^2} + \frac{\partial \mathbf{F}_3}{\partial \zeta} = \mathbf{S}(\mathbf{U}) \Rightarrow \quad \frac{\partial \mathbf{U}}{\partial t} + \nabla \cdot \mathbf{F}(\mathbf{U}) = \mathbf{S}(\mathbf{U})$$

$$\mathbf{U} = \sqrt{G}\begin{bmatrix} \rho' \\ \rho u^1 \\ \rho u^2 \\ \rho w \\ (\rho\theta)' \end{bmatrix}, \quad \mathbf{F}_1 = \sqrt{G}\begin{bmatrix} \rho u^1 \\ \rho u^1 u^1 + p' G_h^{11} \\ \rho u^2 u^1 + p' G_h^{21} \\ \rho w u^1 \\ \rho\theta u^1 \end{bmatrix} \quad \mathbf{F}_2 = \sqrt{G}\begin{bmatrix} \rho u^2 \\ \rho u^1 u^2 + p' G_h^{12} \\ \rho u^2 u^2 + p' G_h^{22} \\ \rho w u^2 \\ \rho\theta u^2 \end{bmatrix}$$

$$\mathbf{F}_3 = \sqrt{G}\begin{bmatrix} \rho\tilde{w} \\ \rho u^1 \tilde{w} + G_v^{13} p' \\ \rho u^2 \tilde{w} + G_v^{23} p' \\ \rho w \tilde{w} + p'/\sqrt{G_v} \\ \rho\theta\tilde{w} \end{bmatrix}, \quad \mathbf{S}(\mathbf{U}) = \sqrt{G}\begin{bmatrix} 0 \\ \sqrt{G_h}\,\rho f(u^1 G^{21} - u^2 G^{11}) - M_\Gamma^1 \\ \sqrt{G_h}\,\rho f(u^1 G^{22} - u^2 G^{12}) - M_\Gamma^2 \\ -\rho' g \\ 0 \end{bmatrix}$$

- Note: M_Γ^1, M_Γ^2 are geometric terms associated with cubed-sphere topology, they have no vertical dependence for shallow atmosphere approximation.

Computational Domain (Horizontal)

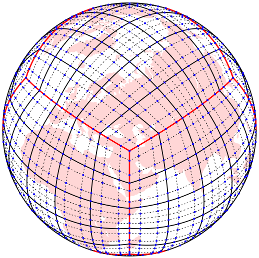

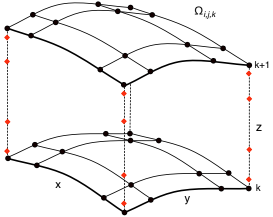

- Dimensional split approach: The computational domain $\mathscr{D}$ is decomposed into 2D + 1D. Independent DG discretization for horizontal (x^1, x^2) cubed-sphere surfaces, and vertical (ζ) direction.
- Cubed-sphere panel is tiled with non-overlapping $N_e \times N_e$ elements, each with $N_p \times N_p$ Gauss quadrature points. This is a standard setup in HOMME framework.
- Horizontal elements are stacked in the vertical direction, which forms the 3D grid system.

Computational Domain (Vertical)

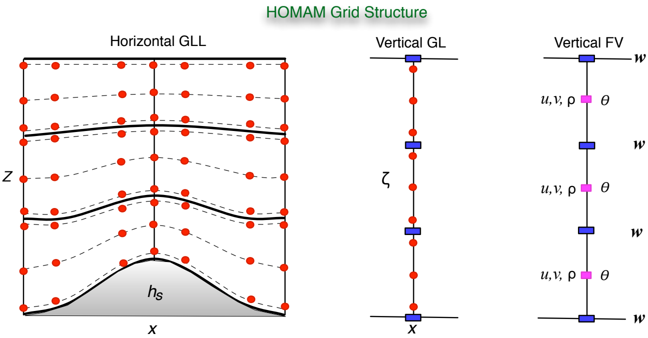

- The vertical grid line z or ζ is partitioned into V_{nel} 1D elements, each with N_g Gauss points. This is a major design change in HOMME/CAM framework.
- Currently Gauss-Legendre (GL) quadrature elements are used in the vertical, which define independent vertical levels with optimal accuracy.
- Total degrees-of-freedom (dof) is $6N_e^2 N_p^2 \times V_{nel} N_g$.
- Other possibilities: High-order FV discretization (WENO, Multi-Moment etc.)

Why DG for spatial discretization?

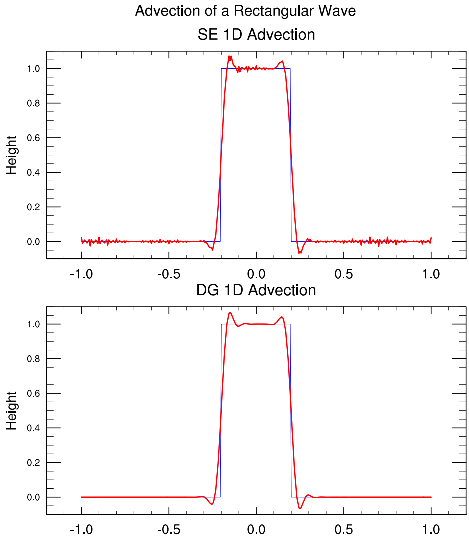

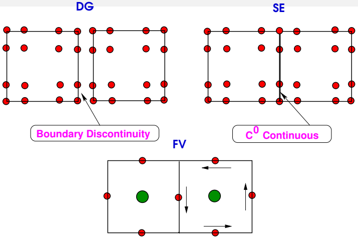

- SE and nodal form of DG use identical GLL grid system. Same MPI communication can be used.
- At element edges SE employs averaging (DSS) which may cause oscillations.
- DG relies on flux operations as in FV method at element edges.
- DG Advantage: Smooth evolution of solution
- DG has about 20% smaller time-step restriction compared to SE with explicit methods.

DG-3D Results

- DG-3D Hydrostatic Dycore (*Nair et al. Comput. & Fluids, 2009*)
- JW-Baroclinic Instability Test, Day 8 Ps ($\approx 1^\circ$ resolution)
- The DG Solution is smooth and free from "spectral ringing".
- HOMME SE version uses hype-diffusion (∇^4), DG version uses LDG diffusion (∇^2)

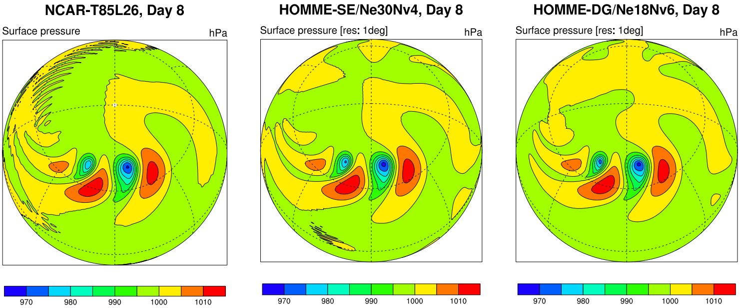

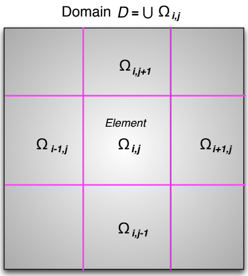

- To Solve:

$$\frac{\partial U_h}{\partial t} + \nabla \cdot \mathbf{F}(U_h) = S(U_h), \quad \text{in } (0,T] \times \mathscr{D}$$

- The domain $\mathscr{D}$ is partitioned into non-overlapping elements Ω_{ij}
- Element edges are discontinuous
- Problem is locally solved on each element Ω_{ij}
- Approximate solution U_h belongs to a vector space $\mathscr{V}_h$ of polynomials $\mathscr{P}_N(\Omega_e)$.

- The Galerkin formulation: Multiplication of the basic equation by a *test function* $\varphi_h \in \mathscr{V}_h$ and integration over an element Ω_e with boundary Γ_e,

$$\int_{\Omega_e} \left[\frac{\partial U_h}{\partial t} + \nabla \cdot \mathbf{F}(U_h) - S(U_h) \right] \varphi_h d\Omega = 0$$

- Weak Galerkin formulation : Integration by parts (Green's theorem) yields:

$$\frac{\partial}{\partial t} \int_{\Omega_e} U_h \, \varphi_h \, d\Omega - \int_{\Omega_e} \mathbf{F}(U_h) \cdot \nabla \varphi_h \, d\Omega \quad + \int_{\Gamma_e} \mathbf{F}(U_h) \cdot \vec{n} \, \varphi_h \, d\Gamma = \int_{\Omega_e} S(U_h) \, \varphi_h d\Omega$$

DG Method: Nodal Spatial Discretization

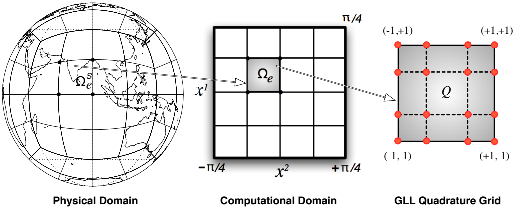

- Every element Ω_e is mapped onto a unique reference element $[-1,1]^2$, with local coordinates $(\xi,\eta) \in [-1,1]$. Grid structure is identical to SE method
- Construct a nodal basis set using a tensor-product of Lagrange polynomials $h_i(\xi)$, with roots at Gauss-Lobatto-Legendre (GLL) or Gauss-Legendre (GL) quadrature points $\{\xi_i\}$.
- The approximate solution and test functions are expressed in terms of basis function:

$$U_h(\xi,\eta) = \sum_{i=0}^{N}\sum_{j=0}^{N} U_{ij}\, h_i(\xi) h_j(\eta) \quad \text{for} \quad -1 \le \xi, \eta \le 1$$

- Final form for the discretization leads to a system of ODEs:

$$\frac{\partial \mathbf{U}}{\partial t} + \nabla \cdot \mathbf{F}(\mathbf{U}) = \mathbf{S}(\mathbf{U}) \quad \Rightarrow \quad \frac{d}{dt}\mathbf{U}_h(t) = \mathscr{L}(\mathbf{U}_h)$$

Time Stepping Challenges for the ODE system

For the resulting ODE systems:

$$\frac{dU_h}{dt} = L(U^h), \quad t \in (0, t_T)$$

where L is the DG spatial discretization operator.

Options & Challenges

- Explicit time integration efficient and easy to implement.
  Stringent CFL constraint $\Rightarrow$ tiny Δt, limited practical value.

$$\frac{C\Delta t}{\bar{h}} < \frac{1}{2N+1}, \quad \bar{h} = \min\{\Delta x, \Delta z\}$$

- Implicit time integration: Unconditionally stable but generally expensive to solve for a 3D model.
- Horizontally Explicit and Vertically Implicit (HEVI). Particularly useful for 3D NH modeling ($\Delta z : \Delta x = 1 : 1000$).
- Practical approach: Split Explicit (e.g. WRF, MPAS, NICAM)

DG-NH Time Stepping with HEVI (Strang-type Split)

- Solve the ODE $d\mathbf{U}/dt = L(\mathbf{U})$ system, where $\mathbf{U} = (\sqrt{G}\rho', \sqrt{G}\rho u^1, \rho u^2, \sqrt{G}\rho w, \sqrt{G}(\rho\theta)')^T$.
- The spatial DG discretization corresponding to $L(\mathbf{U})$ is split into horizontal (H) and vertical (V) components, s.t. $L(\mathbf{U}) = L^H(\mathbf{U}) + L^V(\mathbf{U})$

$$
\begin{aligned}
\mathbf{U}_1 &:= \mathbf{U}_h(t), & \frac{d}{dt}\mathbf{U}_1 &= L^H(\mathbf{U}_1) \quad \text{in } (t, t+\Delta t/2] \\
\mathbf{U}_2 &:= \mathbf{U}_1(t+\Delta t/2), & \frac{d}{dt}\mathbf{U}_2 &= L^V(\mathbf{U}_2) \quad \text{in } (t, t+\Delta t], \\
\mathbf{U}_3 &:= \mathbf{U}_2(t+\Delta t), & \frac{d}{dt}\mathbf{U}_3 &= L^H(\mathbf{U}_3) \quad \text{in } (t+\Delta t/2, t+\Delta t],
\end{aligned}
$$

  and $\mathbf{U}_h(t+\Delta t) = \mathbf{U}_3(t+\Delta t)$.
- Possible options are is to perform "$H-V-H$" sequence of operations and "$V-H-V$" sequence.
- The vertical part may be solved implicitly with DIRK (Diagonally Implicit Runge-Kutta) [1].
- HEVI may be viewed as an IMEX Runge-Kutta (RK) method (Giraldo et al. 2009)
- For the implicit solver:
  - inner linear solver uses Jacobian-Free GMRES.
  - It usually takes 1 or 2 iterations for the outer Newton solver.

[1] Durran, 2010

Time Stepping for 2D Model: Schär Mountain Test-2

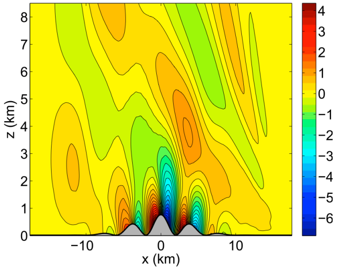

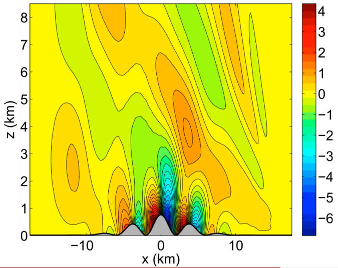

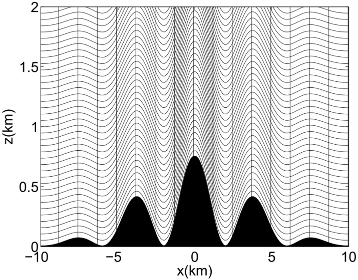

Schemes	Δt (s)	CPU time (s)	Speedup
Explicit	0.04	114.10	1.0
ARS(232)	0.4	71.65	1.6
HEVI	0.4	59.67	1.91

- Ref: *Bao, Kloefkorn & Nair (MWR, 2015)*

3D Advection Test: "Hadley-like" Meridional Circulation

- DCMIP: `https://earthsystemcog.org/projects/dcmip-2012/`, *Kent et al. (2014, QJRMS)*

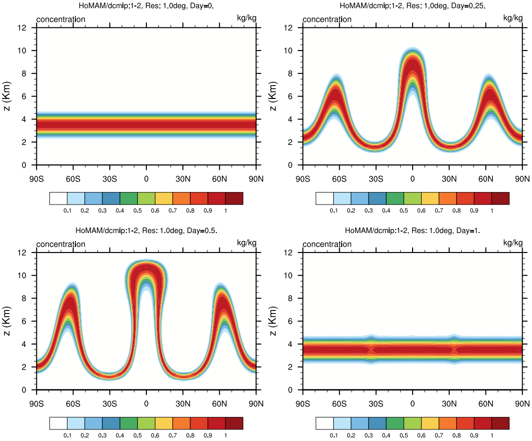

- DCMIP-12: A deformational flow that mimics a "Hadley-like" meridional circulation.
- The wind fields are designed so that the flow reverses itself halfway through the simulation and returns the tracers to their initial position.
- The exact solution is known at the end of the run (1 day).
- HOMAM setup for 1° L60: $N_e = 30$, $N_p = 4$ (GLL); $V_{nel} = 15$; $N_g = 4$ (GL), $\Delta t = 60$ s, 1 day simulation.

- HEVI, HEVE and Full (un-split) produce visually identical results.

3D Advection DCMIP-12 Test: Convergence

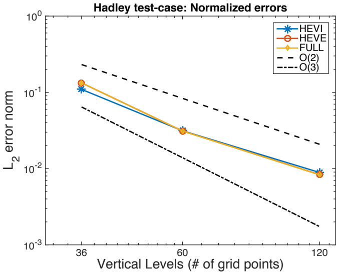

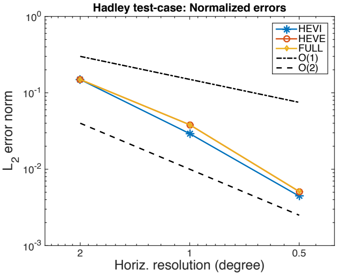

Convergence Rate: *DCMIP, Kent et al. (2014), Hall et al (2016)*

Errors/Models:	Mcore	CAM-FV	ENDGame	CAM-SE	HOMAM
ℓ_1	2.22	1.93	2.18	2.27	2.62
ℓ_2	1.94	1.84	1.83	2.12	2.43
ℓ_∞	1.64	1.66	1.14	1.68	2.16

Table: Average convergence rate for the normalized error norms for the Hadley test (DCMIP test 1-2) computed using resolutions $2^\circ, 1^\circ, 0.5^\circ$ horizontal, and respectively with $30, 60, 120$ vertical levels.

- Temporal convergence is between 1st and 2nd-Order with the Hadley test.

3D Advection: Flow Over Rough Orography (DCMIP-13)

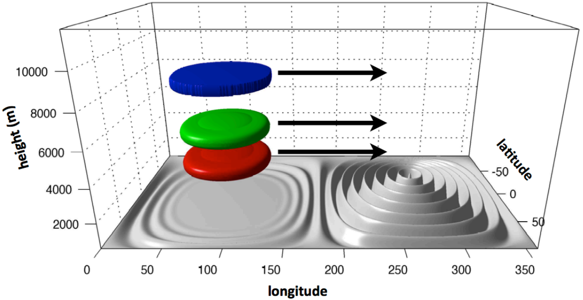

Figure: Schematic for DCMIP-13 test initial condition (*Figure courtesy: David Hall*)

- A series of steep concentric ring-shaped mountain ranges forms the terrain. The prescribed flow field is a constant solid-body rotation (Kent et al., 2014).
- The tracer field q is given by three thin vertically stacked cloud-like patches (non-smooth) which circumnavigate the globe and return to their initial positions after 12 days.

HOMAM: 3D Advection, Flow Over Rough Orography

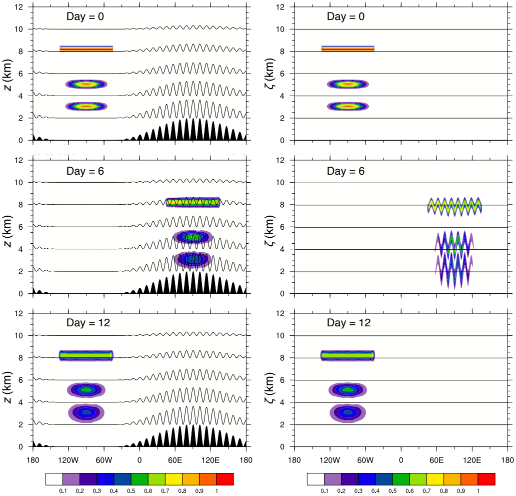

- HOMAM setup for 1° L120: $N_e = 30$, $N_p = 4$ (GLL); $V_{nel} = 30$; $N_g = 4$ (GL), $\Delta t = 6$s, 12 day simulation.

Error Norm	MCore $1^\circ L120$	CAM-SE $1^\circ L120$	HOMAM $1^\circ L120$
ℓ_1	0.83	0.65	0.78
ℓ_2	0.55	0.27	0.50
ℓ_∞	0.73	0.75	0.76

[*Kent et. al. (2014); Hall et al. (2016)*]

- Vertical cross-sections along the equator for the tracer field q = q4 for the DCMIP test
- The results are simulated with HOMAM using the HEVE/HEVI scheme at a horizontal resolution of 1°, 60 vertical levels, and $\Delta t = 12$s.

Preliminary NH Benchmark Test Results with DCMIP

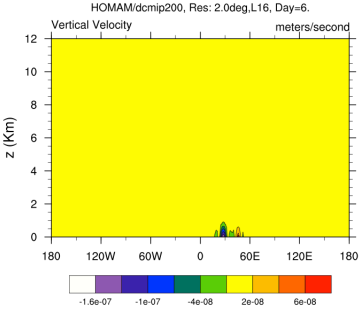

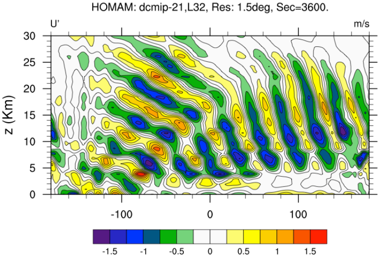

- DCMIP Test 2-0-0: Steady-state hydrostatically-balanced atmosphere at rest, examines the accuracy of the pressure gradient error.
- Regular sized planet, vertical velocity w after 6 days.

- DCMIP Test 2-1: NH mountain waves over a Schär-type Mountain (rough orography) on a reduced planet $(X = 500)$, u' after 3600s
- $N_e = 20, N_p = 4, N_g = 4,\ \Delta t = 0.20$s

HOMAM: Nonhydrstatic Gravity Waves (DCMIP-31)

- NH Gravity Wave test (DCMIP-31) on a reduced planet $(X = 125)$, θ' after 3600s
- $N_e = 25, N_p = 4, N_g = 4$ $(\Delta x \approx \Delta z \approx 1$ km$)$, $\Delta t = 0.20$s
- The initial state is hydrostatically balanced and in gradient-wind balance. An overlaid potential temperature perturbation triggers the evolution of gravity waves.

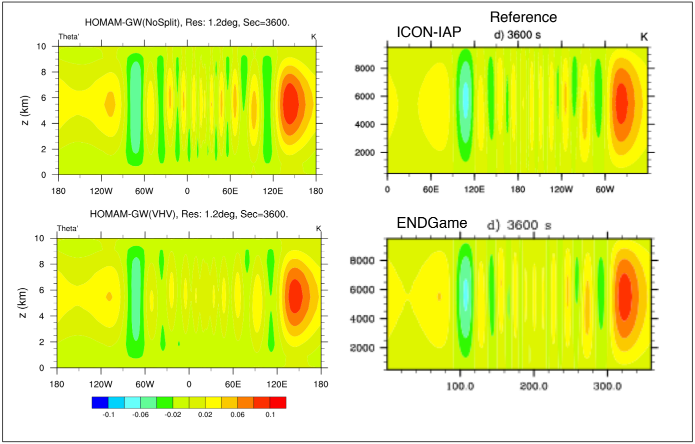

Summary

- Early results with HOMAM Dycore (split and unsplit) are promising, and it performs well under benchmark test cases.
- Accuracy of the operator-split DG is acceptable.
- HEVI effectively relaxes the CFL constraint to the horizontal dynamics only, and permits significantly larger time step as opposed to the fully explicit method.
- The 3D advection convergence shows a second-order accuracy with the smooth scalar field, irrespective of a particular time-integrator (HEVI, HEVE or un-split).

Future Work (WIP)

- Improve the efficiency of HEVI time-stepping (efficient pre-conditioner for implicit part).
- Test Split-Explicit method, employ multi-rate time integration scheme (subcycling).
- Latest DCMIP tests & ultimately CAM integration.

Thank You!